

## Direct reactions for nuclear structure required for fundamental symmetry tests

P. E. Garrett<sup>1,a</sup>, E. T. Rand<sup>1</sup>, A. Diaz Varela<sup>1</sup>, G.C. Ball<sup>2</sup>, V. Bildstein<sup>1</sup>, T. Faestermann<sup>3</sup>, B. Hadinia<sup>1</sup>, R. Hertenberger<sup>4</sup>, D. S. Jamieson<sup>1</sup>, B. Jigmeddorj<sup>1</sup>, K. G. Leach<sup>1,5</sup>, C. E. Svensson<sup>1</sup>, and H.-F. Wirth<sup>4</sup>

<sup>1</sup>Department of Physics, University of Guelph, Guelph, ON, N1G2W1 Canada

<sup>2</sup>TRIUMF, 4004 Wesbrook Mall, Vancouver, BC V6T2A3 Canada

<sup>3</sup>Physik Department, Technische Universität München, D-85748 Garching, Germany

<sup>4</sup>Fakultät für Physik, Ludwig-Maximilians-Universität München, D-85748 Garching, Germany

<sup>5</sup>Department of Physics, Colorado School of Mines, Golden CO, 80401 USA

**Abstract.** A program of nuclear structure studies to support fundamental symmetry tests has been initiated. Motivated by the search for an electric dipole moment in  $^{199}\text{Hg}$ , the structure in the vicinity has been explored via direct reaction studies. To date, these have included the  $^{198,200}\text{Hg}(d, d')$  inelastic scattering reactions, with the aim to obtain information on the  $E2$  and  $E3$  strength distributions, and the  $^{198}\text{Hg}(d, p)$  and  $^{200}\text{Hg}(d, t)$  reactions to obtain information on the single-particle states in  $^{199}\text{Hg}$ . The studies using the  $^{200}\text{Hg}$  targets have been fully analyzed using the FRESKO reaction code yielding the  $E2$  and  $E3$  strength distribution to 4 MeV in excitation energy, and the  $(d, t)$  single-particle strength to over 3 MeV in excitation energy.

### 1 Introduction

The combination of charge-conjugation ( $C$ ) and parity ( $P$ ) violating processes is essential for the explanation of the matter-antimatter asymmetry observed in the Universe [1]. The  $CPT$  Theorem [2] states that invariance under transformations of the combination of the three fundamental symmetries,  $C$ ,  $P$ , and time-reversal transformation ( $T$ ) is strictly obeyed. To date, all experimental evidence supports that  $CPT$  is a true symmetry of nature, and thus a violation of  $CP$ , as required for baryogenesis, implies  $T$  violation. A particle electric dipole moment (EDM) is odd under both the  $P$  and  $T$  transformations, therefore a permanent EDM for an elementary particle or atom can only arise from parity *and* time-reversal violating fundamental interactions.

The Standard Model sources of  $CP$  violation, in the weak interaction represented by the complex phase  $\delta_{\text{CKM}}$  of the Cabibbo-Kobayashi-Maskawa (CKM) matrix, and in a phase that arises from the vacuum expectation value of the quantum chromodynamics (QCD) gluon field  $\delta_{\text{QCD}}$ , are insufficient to account for the matter-antimatter asymmetry. Additional sources of  $CP$  violation are therefore required, providing a strong motivation to search for new  $CP$ -violating physics beyond the Standard Model. Present theories beyond the Standard Model, such as multiple-Higgs theories, left-right symmetric, and supersymmetry (SUSY), generally predict EDMs within current experimental reach [3]. Furthermore, present upper limits on the EDMs of the neutron, electron and  $^{199}\text{Hg}$  atom have al-

ready significantly reduced the parameter spaces of these models. Currently, the upper limit on the EDM of the  $^{199}\text{Hg}$  atom provides the most stringent limit on many possible  $CP$ -violating terms [4]. Measuring an EDM in a neutral atom is complicated by orbiting atomic electrons, which would arrange themselves to exactly cancel an EDM if the nucleus were a point-like object. Fortunately, nuclei have a finite size and the screening effect does not completely cancel the observable atomic EDM. The intrinsic Schiff moment, the lowest order time-reversal odd moment of a nucleus that is measurable in a neutral atom [5], is a measure of the difference between the charge and dipole distributions of the nucleus. It is responsible for inducing the observable atomic EDM in the electron cloud of the atom. To gain a better understanding of the distribution of Schiff strength in  $^{199}\text{Hg}$ , higher precision data on the  $E1$ ,  $E2$ , and  $E3$  strength distributions are required.

With the aim of providing greater knowledge of the electric strength distributions in the Hg isotopes than is currently available, a program of study of the inelastic scattering reactions has been initiated, with  $^{200}\text{Hg}$  the first nucleus studied. Inelastic scattering provides information on nuclear matrix elements, including those for high multipolarities that typically cannot be obtained in Coulomb excitation experiments employing  $\gamma$ -ray detection. Additionally, nucleon transfer reactions are being re-investigated with the aim of achieving higher sensitivity and information on states at higher excitation energy.

The Hg experimental program represents an expansion of an on-going program of direct reaction studies moti-

<sup>a</sup>e-mail: [pgarrett@physics.uoguelph.ca](mailto:pgarrett@physics.uoguelph.ca)

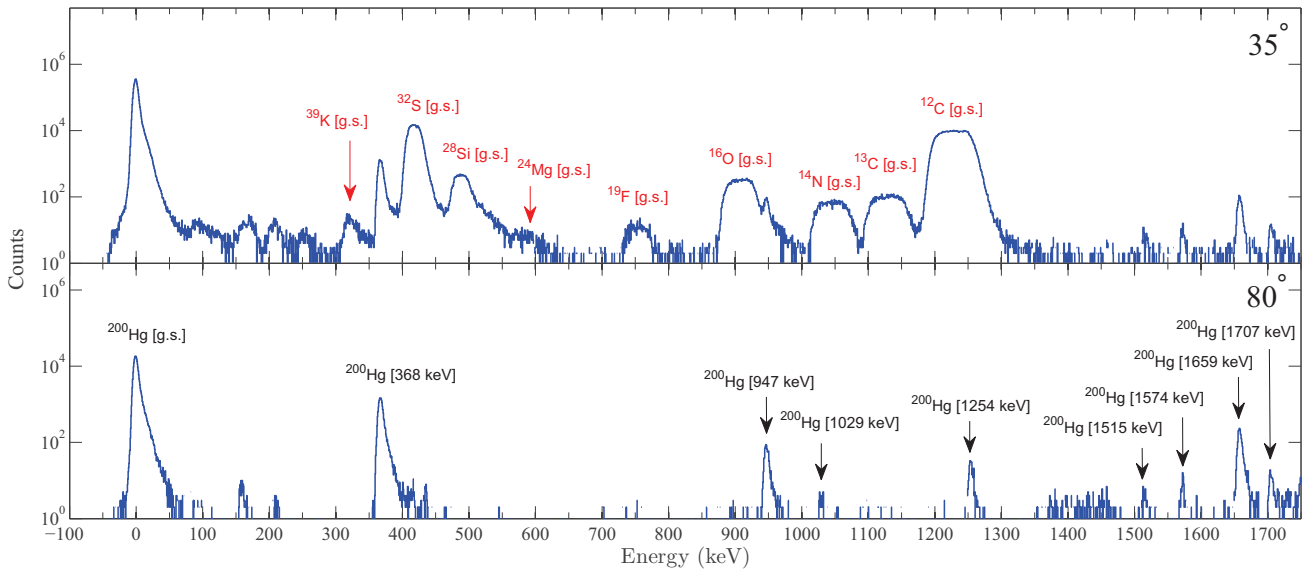


**Figure 1.** Portion of the spectrum obtained at 35° (top) and 80° (bottom) from the bombardment of the  $^{200}\text{Hg}^{32}\text{S}$  target with 22 MeV deuterons. The deuterons originating from the light-mass impurities, having different kinematics and focusing properties than those from the  $^{200}\text{Hg}$ , can be identified by their width and movement as a function of angle with respect to the  $^{200}\text{Hg}$  peaks. This high-energy portion of the deuteron spectrum has many of the light-mass impurity labelled by their origin in the top panel; at high scattering angles these light-mass impurity peaks are no longer present in the spectrum which reveals a number of lower-intensity  $^{200}\text{Hg}$  peaks from inelastic scattering.

vated by fundamental symmetry tests, especially daughter nuclei of superallowed Fermi  $\beta$  emitters. For example, one- and two-neutron transfer measurements on  $^{52}\text{Cr}$  and  $^{64}\text{Zn}$  related to the superallowed Fermi decays of  $^{50}\text{Mn}$  and  $^{62}\text{Ga}$  have been performed [6–8]. These studies highlight the power of combining different techniques and the complementarity of studies for fundamental symmetries and nuclear structure.

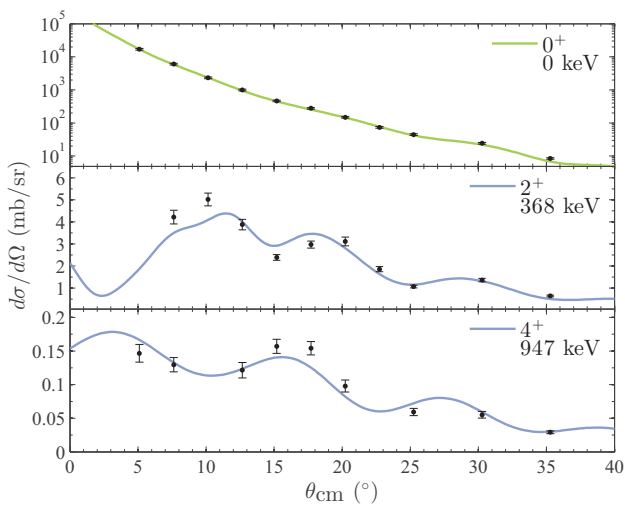


**Figure 2.** Angular distributions obtained for the  $^{200}\text{Hg}(d, d')$  reaction with 22 MeV deuteron beams. The top panel displays the elastic scattering cross sections, the middle panel the inelastic cross section to the  $2_1^+$  state, and the bottom panel the cross sections for excitation of the  $4_1^+$  state. The curves are the results of coupled-channel calculations performed with the FRESKO code.

## 2 Experimental details and results

The experiments to investigate reactions on targets of  $^{200}\text{Hg}$  were performed at the Maier-Leibnitz Laboratorium of the Ludwig-Maximilians Universität München and the Technische Universität München. Beams of 22 MeV deuterons up to 1  $\mu\text{A}$  of current bombarded targets of  $^{200}\text{Hg}^{32}\text{S}$  of varying thicknesses, but generally on the order of 100  $\mu\text{g}/\text{cm}^2$  of  $^{200}\text{Hg}$ . The products of the reaction were momentum analyzed with a Q3D spectrograph employing a position-sensitive focal-plane detector that also provided signals used for  $\Delta E$  vs.  $\Delta E$  and  $\Delta E$  vs.  $E$  for particle identification. The HgS compound was sandwiched between two C foils of 12  $\mu\text{g}/\text{cm}^2$  thickness. While care was taken to minimize the quantity of impurities that the target material was exposed to, as shown in Fig. 1 several impurities beyond the usual appearance of atmospheric gases and  $^{28}\text{Si}$  were still observed, albeit for many at the level of a few parts per  $10^4$  or  $10^5$ . Due to the differences in the kinematics of the deuterons scattering from these light-mass targets vs. the heavy  $^{200}\text{Hg}$ , the apparent positions of the peaks move in the spectrum to positions corresponding to high Hg excitation energies as the scattering angle increases, and the peaks themselves become increasingly wide as the target mass decreases.

Figure 2 displays the angular distributions obtained for elastic scattering, and excitation of the  $2_1^+$  and  $4_1^+$  levels. The smooth curves are results of coupled-channel calculations performed with the FRESKO code [9] using optical model parameters of Daehnick *et al.* [10]. (Different global optical model parameter sets were tested, but the Daehnick *et al.* [10] set provided the best reproduction of the elastic scattering data.) The results of the present

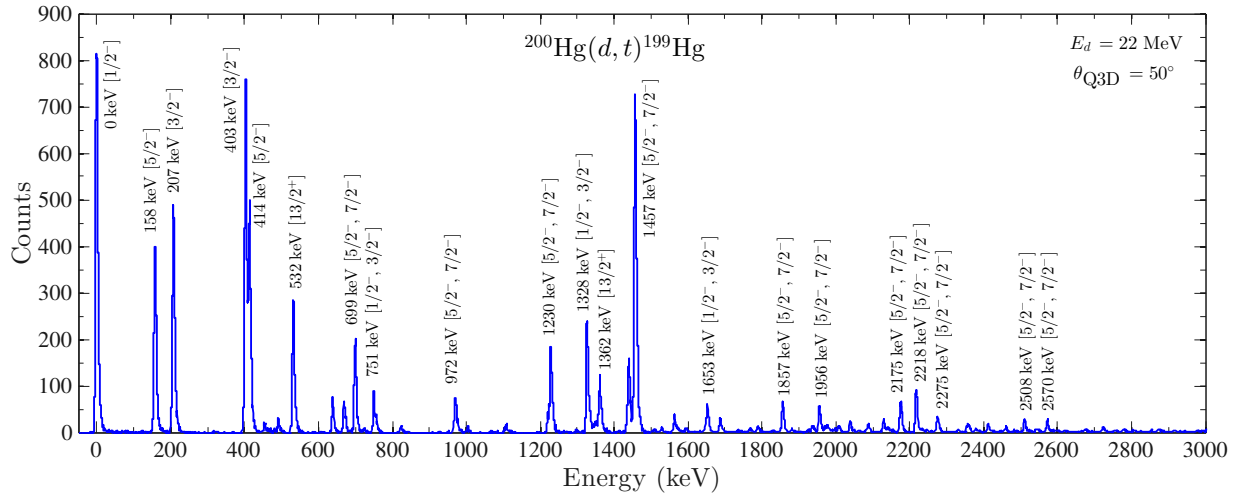


**Figure 3.** Portion of the triton spectrum observed at an angle of  $50^\circ$  following the  $^{200}\text{Hg}(d,t)^{199}\text{Hg}$  reaction with 22 MeV deuterons. Some of the more prominent peaks are labelled with their corresponding excitation energies in  $^{199}\text{Hg}$  and the state  $I^\pi$  values.

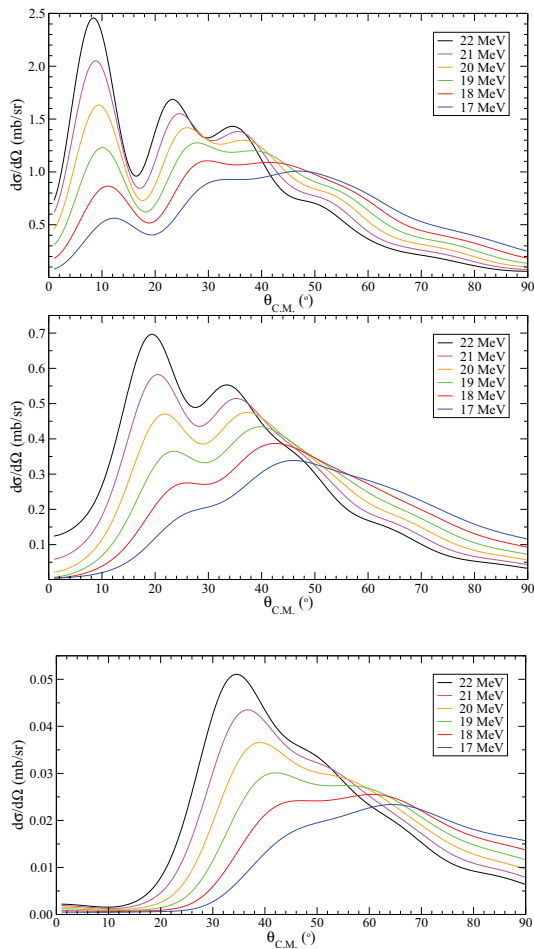


**Figure 4.** Calculated  $^{200}\text{Hg}(d,t)^{199}\text{Hg}$  angular distributions for the  $l = 1$  transition to the  $1/2^-$  ground state (top), for  $l = 3$  to the 158-keV  $5/2^-$  state (middle), and for  $l = 6$  to the 532-keV  $13/2^+$  state (bottom) for the deuteron beam energies indicated.

work are generally in good agreement with previous results as listed in the Nuclear Data Sheets [11]. The values of  $\beta_2 = 0.116(12)$  for excitation of the  $2_1^+$  level, and  $\beta_2 = 0.082(8)$  and  $\beta_4 = 0.013(3)$  for excitation of the  $4_1^+$  level were determined. As Fig. 2 shows, very good fits to the data were obtained. The previously assigned  $3^-$  states at 2151 keV and 2609 keV were observed, and a number of higher-lying states were favoured to be  $3^-$  states as well. The  $3_2^-$  level was the strongest populated, with the  $3_1^-$  level a factor of 7 weaker and the remaining  $3^-$  states weaker still.

Figure 3 shows the spectrum obtained at  $50^\circ$  for the  $^{200}\text{Hg}(d,t)^{199}\text{Hg}$  reaction with 22 MeV deuterons. An excellent resolution of 7 keV full width at half maximum was achieved enabling, for example, the separation of the 403- and 414-keV states. Compared to the previous work by Moyer [12], the angular distributions obtained in the present study have a much enhanced diffraction pattern, allowing the better determination of the transferred  $l$  value. Figure 4 displays the calculated angular distributions at incident deuteron beam energies from 17 MeV to 22 MeV for the  $I^\pi = 1/2^-$  ground state, populated by an  $l = 1$  transfer, the  $I^\pi = 5/2^-$  158-keV state, populated by an  $l = 3$  transfer, and the  $I^\pi = 13/2^+$  532-keV state, populated by an  $l = 6$  transfer. The experimental angular distributions for these corresponding states are shown in Fig. 5 with the calculated angular distributions. Excellent agreement between the experimental data and the theoretical curves are observed. From the fits to the data, the spectroscopic strengths, defined by

$$S_{jl} = \frac{\left. \frac{d\sigma}{d\Omega} \right|_{\text{exp}}}{\left. \frac{d\sigma}{d\Omega} \right|_{\text{s.p.}}} \quad (1)$$

are extracted where  $\left. \frac{d\sigma}{d\Omega} \right|_{\text{s.p.}}$  is the calculated single-particle cross section using the FRESKO code, and optical model

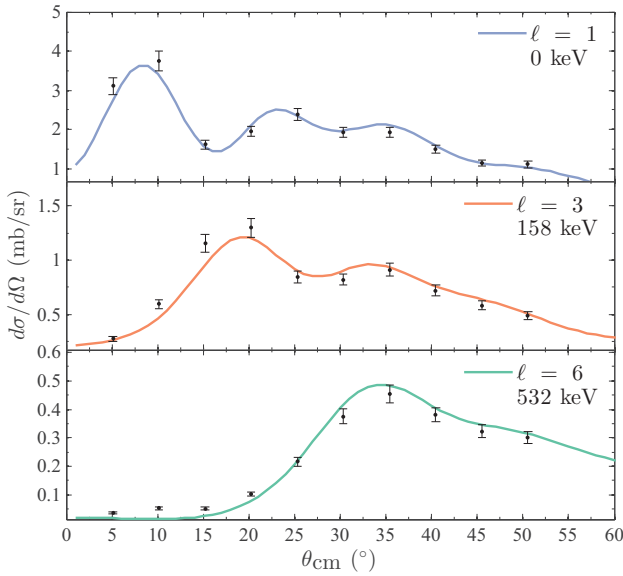


**Figure 5.** Observed  $(d, t)$  angular distributions for population of the  $^{199}\text{Hg}$   $1/2^-$  ground state (top), 158-keV  $5/2^-$  (middle) and 532-keV  $13/2^+$  (bottom). The curves are results of FRESKO calculations for the transferred  $l$  value indicated.

parameters from Refs. [10] and [13] for the deuterons and tritons, respectively.

In total, 91 states, of which 50 were newly discovered, in  $^{199}\text{Hg}$  were observed up to an excitation energy of approximately 3 MeV. Of these 50 new levels, 22 have definitely assigned transferred  $l$  values, with a further 15 previously identified levels also having firm transferred  $l$  values. For the remaining levels, their population is so weak that definite assignments could not be made. The spectroscopic strengths extracted for  $l = 1$ ,  $l = 3$ , and  $l = 6$  transfer were combined with previous results from the  $^{200}\text{Hg}(d, p)$  reaction by Moyer [12] to test the sum rule. The sum rule for a specific single-particle orbital with angular momentum  $j$  is

$$\sum_{\text{pickup}} S_{jl} + \sum_{\text{stripping}} (2j + 1) S_{jl} = 2j + 1 \quad (2)$$

if all possible single-particle strength is observed. Since no distinction can be made between the  $l = j \pm 1/2$  transfers, the combined sum rule for  $l = 1$  transfer should be equal to 6, for  $l = 3$  it should yield 14, and for  $l = 6$  it should equal 14. The experimentally observed sums are 6.4,  $\approx 11$ , and 14, respectively, each with approximately 20% uncertainty. Thus, all the expected strength has been observed, except for a small amount of  $l = 3$  strength.

### 3 Summary

New experiment data on  $(d, d')$  inelastic scattering on targets of  $^{200}\text{Hg}$  have been obtained and analyzed with the FRESKO coupled-channel code. The new data indicate that the  $3_2^-$  level at 2609 keV is the strongest populated  $3^-$  state, accounting for at least 50% of the observed  $3^-$  excitation strength. In addition, new results obtained for the  $^{200}\text{Hg}(d, t)^{199}\text{Hg}$  reaction has located nearly all of the  $p_{1/2,3/2}$ ,  $f_{5/2,7/2}$ , and  $i_{13/2}$  single-particle strength. Similar data on targets of  $^{198}\text{Hg}$  are currently under analysis, and future work will include inelastic scattering studies on targets of  $^{199}\text{Hg}$  and  $\gamma$ -ray spectroscopy to elucidate the  $E1$  strength in low-lying levels of the Hg isotopes.

### Acknowledgements

This work was supported in part by the Natural Sciences and Engineering Research Council (Canada). TRIUMF receives federal funding via a contribution agreement through the National Research Council of Canada.

### References

- [1] A. D. Sakharov JETP Lett. **5**, 24 (1967).
- [2] M. E. Peskin and D. V. Schroeder, *An Introduction To Quantum Field Theory (Frontiers in Physics)* (Westview Press, 1995), ISBN 0201503972.
- [3] J. Pendlebury and E. Hinds, Nucl. Instrum. Meth. **A440**, 471 (2000).
- [4] B. Graner, Y. Chen, E. G. Lindahl, and B. R. Heckel, arXiv:1601.04339 [physics.atom-ph].
- [5] V. V. Flambaum and V. G. Zelevinsky, Phys. Rev. C **68**, 035502 (2003).
- [6] K. G. Leach, P.E. Garrett, G.C. Ball *et al*, Phys. Rev. C **94**, 011304(R) (2016).
- [7] K. G. Leach, P. E. Garrett, I. S. Towner, *et al*, Phys. Rev. C **87**, 064306 (2013).
- [8] K. G. Leach, P. E. Garrett, C. E. Svensson *et al*, Phys. Rev. C **88**, R031306 (2013).
- [9] I. J. Thompson, Comp. Phys. Rep. **7**, 167 (1988).
- [10] W. W. Daehnick, J. D. Childs, and Z. Vrcelj, Phys. Rev. C **21**, 2253 (1980).
- [11] F. Kondev and S. Lalkovski, Nucl. Data Sheets **108**, 1471 (2007).
- [12] R. Moyer, Phys. Rev. C **5**, 1678 (1972).
- [13] X. Li, C. Liang, and C. Cai, Nucl. Phys. **A789**, 103 (2007).